Thermal displacements of concrete dams: Accounting for water temperature in statistical models

Maxime Tatin, Matthieu Briffaut, Frédéric Dufour, Alexandre Gilles Simon, Jean-Paul Fabre

Thermal displacements of concrete dams: Accounting for water temperature in statistical models

M. Tatin [a,b,c,*], M. Briffaut [a,b], F. Dufour [a,b], A. Simon [c], J.-P. Fabre [d]

[a] Univ. Grenoble Alpes, 3SR, F-38000 Grenoble, France
[b] CNRS, 3SR, F-38000 Grenoble, France
[c] EDF DTG, 21 avenue de l'Europe, BP41, 38000 Grenoble, France
[d] EDF DTG, 62 Bis rue Raymond IV, BP875, 31685 Toulouse Cedex 6, France

Measurements of concrete dam displacements are influenced by various factors such as hydrostatic load, thermal effect and irreversible phenomena (creep, swelling, etc.). To interpret measurements and improve the assessment of irreversible effects, splitting the different influences is necessary. For this purpose, models based on statistics and physics are commonly employed in engineering studies. Although they are efficient in most cases to analyse the displacement of concrete dams, these models are built on a certain number of hypotheses, necessary to write "simple" mathematical relationships, but leading to uncertainties. To evaluate the suitability of these physico-statistical models (importance of the hypotheses) and to improve it, a 2D finite element (FE) model has been developed as a heuristic case. This study shows the importance of water temperature and temperature gradient in the assessment of the thermal displacements. So, a new physico-statistical model is proposed to account for these phenomena. The evaluation of its performance on both the FE heuristic case and real cases shows that the improved assessment of thermal effects on reversible phenomena leads to a reduced uncertainty on residuals. Thus, the proposed approach yields to a better assessment of irreversible trends.

1. Introduction

Safety is an important issue for dam management. As the structural vulnerability increases with the dam ageing, it is essential to monitor dams for ensuring their safety over the long term. Dam surveillance mainly consists of analysing gathered data in order to verify that the dam is functioning as intended, to detect any possible anomalies, and to warn of any change which could endanger its safety. Displacements, pressure and flow rates are classical measures for dam safety.

This contribution focuses on dam displacement analysis. Although a lot of instruments (e.g. collimators, laser, radar, etc.) can be employed, dam displacements are generally measured by direct or invert pendulums. They are influenced by several factors such as hydrostatic load, thermal conditions and irreversible phenomena (creep, alkali-aggregate reaction, adaptation, consolidation, damage, cracking, etc.). The simplest analysis consists in plotting measured displacements as a function of time, or as a function of the reservoir level, but this type of graph is difficult to analyse because of dispersion due to external reversible influences (thermal and filling conditions). Usually, in one year, the irreversible part of the displacement is less than 1% of the reversible displacement (e.g. for a 130 m height arch dam, the thermal displacements amplitude is about 20 mm, whereas its irreversible trend is about 0.1 mm per year). As a consequence, statistical models are commonly used to separate the influences of the different explicative factors, and then to observe anomalies or irreversible trends.

Statistical modelling is a classical approach in data analysis and is employed in various domains [1]. A statistical model is a mathematical formulation of the existing relationships between environmental factors (water level, temperatures) and dam behaviour (displacements, pressure, flow). By calibrating these models on the past behaviour of the dam, a diagnostic can be established on the recent behaviour which is expected to remain the same.

The most common statistical method in dam engineering is called HST (Hydrostatic, Season, Time) and has been developed by EDF (Électricité De France) in the 1960s [2–4]. With this model,

* Corresponding author at: Univ. Grenoble Alpes, 3SR, F-38000 Grenoble, France. Tel.: +33 6 71 56 35 63.
E-mail addresses: maxime.tatin@3sr-grenoble.fr (M. Tatin), matthieu.briffaut@3sr-grenoble.fr (M. Briffaut), frederic.dufour@3sr-grenoble.fr (F. Dufour), alexandre-gilles.simon@edf.fr (A. Simon), jean-paul.fabre@edf.fr (J.-P. Fabre).

the reversible influences can be assessed (hydrostatic and seasonal components) and subtracted to the measurements so as to highlight the irreversible behaviour of the dam. For several decades, the obtained results have confirmed the relevance and soundness of this method for interpretation of dam monitoring measurements [5–7]. This method is currently used in several countries [8–12].

However, in the HST model, thermal displacements are assumed to follow a perfectly seasonal evolution (one-year period harmonic function). As a consequence, the performance of HST is not always sufficient, particularly when time periods are significantly colder or warmer than seasonal average. For a majority of concrete dams, thermal displacements induce a large proportion of the recorded displacement. Thus, it is really important to identify this component accurately while interpreting newly recorded data [13,14].

Several approaches have been proposed to improve the modelling of the thermal influence by accounting for real temperature evolution. Statistical models that considered explicitly data from thermometer embedded in the concrete mass have been proposed [15,13]. Using directly concrete temperature measurements as explicative factors allows avoiding uncertainties due to heat transfer processes, especially at the boundaries. However, the thermometers give local informations which are not totally representative of the global temperature field. Thus, more sophisticated models have been developed to express the temperature field in term of linear effective temperature across the dam cantilever sections [13,16]. The approximation of the non-linear one-dimensional thermal field along the thickness of the dam by a linear equivalent one is considered as sufficient to estimate the global displacements [17,14,13,16]. Then, the temperature field along a cross section can be represented by its mean and its gradient. In these methods, an inverse heat transfer problem is employed to obtain the temperatures at the boundaries from temperatures recorded by the embedded thermometer and a direct heat transfer problem to rebuilt the linear effective temperature from the boundary temperatures. These statistical models, based on a deterministic structural calculation (the thermal variables), are called "hybrid" models in opposition to "purely statistical" (e.g. HST model) or "purely deterministic" models (e.g. finite element (FE) model).

Besides, after the exceptional 2003 European heatwave, a model based on the exploitation of the air temperature instead of internal thermometer (which are not available for the majority of dams) has been developed [18]. The model, called HSTT (Thermal HST) is an hybrid model, it keeps the seasonal function of HST but adds a corrective term which accounts for delayed deviation of the daily air temperature to its seasonal average. This method enables to reduce significantly the residual dispersion of the HST model and reduces the anomalies induced by exceptional thermal conditions.

Nevertheless, since water temperature, solar radiation and coupling phenomena such as thermal boundary conditions depending on the reservoir level are not directly taken into account (the influence of these phenomena on the displacement can be partially captured by the seasonal function), the thermal state of the structure cannot be correctly assessed. Moreover, in the HSTT approach, the thermal state of the structure is reduced to the estimation of the mean temperature. However, according to [14,13,16], the mean temperature but also the temperature gradient across the dam are important for calculating the global displacements. For all these reasons, the residual dispersion of the model may remain high in some cases (some few tenths of millimetres) and the irreversible behaviour difficult to appreciate.

The objective of this study is to improve the assessment of the thermal displacements in the statistical analysis and thus to reduce the residual dispersion. A previous study has identified water temperature as an important source of dispersion for the HSTT model [19]. Based on this analysis, a new physico-statistical model has been developed by taking into account water temperature (and the temperature gradient generated by the difference between air and water temperature). This new hybrid model will be presented after a brief presentation of the HSTT model. Besides, a 2D finite element model of a gravity dam has been developed and will be considered as a heuristic case. Based on thermo-mechanical simulations, this model allows us to separate numerically the different thermal influences and will be employed to validate the capability of the new model to capture the thermal effect induced by water temperature and to compare its performance to HSTT. Finally, the new model will be validated on real monitoring data for several dams.

2. The HSTT model

HSTT is a hybrid physico-statistical model [18]. Its objective is to decompose the measurements in a sum of reversible and irreversible influences to appreciate the behaviour of the dam. Each influence is modelled by a mathematical expression. The global model is a multi-linear regression formed by the sum of all the expressions and is adjusted on the measurements by the least square method. The HSTT model decomposes the displacements into three components:

- A time-dependent irreversible component which represents the long term behaviour of the dam (creep, adaptation, swelling, consolidation, settling, etc.). Although exponential functions can be used (to represent the evolution of concrete creep at early age), for the sake of simplicity, irreversible phenomena are modelled in this contribution by a linear function of the time t (it is assumed on the analysis period chosen in this study that the creep phenomenon is cushioned):

$$f_1(t) = a_1 \cdot t \tag{1}$$

- A hydrostatic reversible component which represents the displacements due to hydrostatic loading. It is modelled as a fourth degree polynomial function of the variable $z = \frac{RN-h}{RN-R_{empty}}$ (RN is the normal reservoir level, R_{empty} is the empty reservoir level and h is the actual reservoir level):

$$f_2(z) = a_2 \cdot z + a_3 \cdot z^2 + a_4 \cdot z^3 + a_5 \cdot z^4 \tag{2}$$

- A thermal reversible component which represents dam displacements due to temperature variations. This component is decomposed into two functions:
  - A seasonal function which represents the thermal displacements induced by the seasonal part of thermal loads. The dam response to seasonal phenomena is assumed to follow periodic evolution of period one year. Thus, this seasonal influence is modelled by the two first terms of the Fourier series decomposition of a one year periodic signal. Accounting for the second term of the Fourier series generally improves the statistical analysis as there is seasonal but non-harmonic thermal phenomena (e.g. water temperature, solar radiation). So, the seasonal function is the sum of harmonic functions of the season angle S (the angle S linearly increases by 2π rad in one year):

$$f_3(S) = a_6 \cdot cos(S) + a_7 \cdot sin(S) + a_8 \cdot cos(2 \cdot S) + a_9 \cdot sin(2 \cdot S) \tag{3}$$

    It is worth noting that this seasonal function is the same than the one used in the HST model. Nevertheless, another form of this function can be found in the literature (e.g.

[3]: $f_3^*(S) = a_6 \cdot cos(S) + a_7 \cdot sin(S) + a_8 \cdot sin^2(S) + a_9 \cdot sin(S) \cdot cos(S)$). The development of this last formulation using trigonometric formula shows that the two functions $f_3(S)$ and $f_3^*(S)$ are almost equivalent, only the mean values over one year of the functions are different (null for $f_3(S)$ and not null for $f_3^*(S)$). For this reason, the function $f_3(S)$ is generally preferred.

- A corrective function which accounts for the delayed response of the structure to daily air temperature:

$$f_4(\Delta\theta_R) = a_{10} \cdot \Delta\theta_R \tag{4}$$

Compared to the HST model, the addition of a corrective term $\Delta\theta_R$ enables a better explanation of the displacements measured during abnormal climatic events at the cost of the estimation of air temperature to feed the model. The daily air temperature signal θ is decomposed as the sum of two signals:

- The average seasonal air temperature θ_S.
- The deviation $\Delta\theta$ of the air temperature to its seasonal average.

The thermal displacement induced by the average seasonal air temperature θ_S is assumed to be seasonal and is thus captured by the seasonal function $f_3(S)$, whereas the thermal displacement induced by the air temperature deviation $\Delta\theta$ is captured by the corrective function $f_4(\Delta\theta_R)$.

The variable $\Delta\theta_R$ is a lagged variable of the air temperature deviation $\Delta\theta$. It is calculated by means of a one-dimensional conductive heat-transfer problem. $\Delta\theta_R$ is the mean temperature of a one dimensional medium with the air temperature deviation applied at its two boundaries. This term is evaluated by convolving the signal of the air temperature deviation $\Delta\theta$ with the impulse response (in term of mean temperatures) of the 1D medium. The convolution product can be estimated by using Eqs. (5) and (6) (see Appendix B for more details):

$$\Delta\theta_R(t) = \frac{8}{\pi^2 \cdot T_0} \cdot \sum_{\substack{n \geq 1 \\ nodd}} X_n(t) \tag{5}$$

In Eq. (5) each term of the sum is calculated through a recurrence formula:

$$X_n(t + \Delta t) = \Delta\theta(t + \Delta t) \cdot \frac{T_0}{n^2} \cdot \left(1 - e^{-n^2 \frac{\Delta t}{T_0}}\right) + X_n(t) \cdot e^{-n^2 \frac{\Delta t}{T_0}} \tag{6}$$

In Eqs. (5) and (6), the term T_0 is the characteristic time representing the thermal inertia of the structure. This parameter T_0 is a statistical parameter of the model.

From a practical point of view, a finite number of terms of the infinite sum (Eq. (5)) has to be considered to compute the lagged variable $\Delta\theta_R$. The first terms of the sum are those which account for the lower frequencies of the thermal loads. Increasing the number of terms will lead to a more accurate solution by accounting for higher frequencies of the input signal at the cost of a larger computational time. Generally, in engineering, only the first term is considered [18]. This is acceptable for thick structures like dams where the high frequencies of thermal loads do not have a major effect on the global thermal state of the structure. Nevertheless, the solution can be slightly improved by adding additional terms. A parametric study has been performed to find the optimal number of terms (compromise between accuracy of the solution and cost in term of computational resources). This parametric study has been performed on the three heuristic displacements time series (see Section 4). The results (Fig. 1) show that, for the three simulations developed in Section 4, the residual dispersion can be reduced by adding more terms in the impulse response, until an asymptotic behaviour. For this study, the optimal value has been arbitrarily chosen around 15. Adding more than 15 terms does not improve significantly the performance of the model. Thus, the results presented in the following of this paper have been computed using 15 terms.

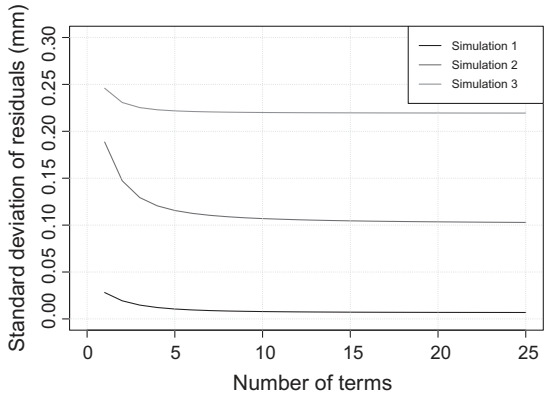

Fig. 1. Evolution of the HSTT residual dispersion with the number of terms.

At the end, the HSTT model can be written as follows:

$$\delta = a_0 + f_1(t) + f_2(z) + f_3(S) + f_4(\Delta\theta_R) + \varepsilon \tag{7}$$

where δ is the measured displacement signal, a_0 is a constant which represents the displacement at the beginning of the analysis, and ε is the residuals of the model which contain uncertainties of both the experimental measurements and the model (the part of residuals due to the experimental measurements is very small compared to the one of the model). In Eq. (7), the eleven coefficients from a_0 to a_{10} of the four functions f_1 to f_4 (Eqs. (1)–(4)) are adjusted statistically on measurements by the least square method.

3. Original development of a new hybrid physico-statistical model: HST-Grad

Although a part of the effect induced by water temperature can be captured by its seasonal function, HSTT does not explicitly account for water temperature. Water temperature has been identified as an important source of dispersion for the HSTT model [19]. Indeed, water temperature is not perfectly seasonal and its contribution to thermally induced displacement is dependent on the retention level. Moreover, water temperature highly contributes to the establishment of a thermal gradient through the structure. The HSTT approach is limited to the estimation of the mean temperature through the lagged variable $\Delta\theta_R$ whereas, the mean temperature but also the temperature gradient are important for calculating the global displacements. In this section, a new original model is proposed by taking explicitly into account water temperature in the HSTT approach. The new hybrid model, called HST-Grad (like temperature GRADient), considers both the mean temperature and the temperature gradient.

Based on the hypotheses of Appendix A, the thermal displacement δ_{th} of the dam can be assessed according to Eq. (8).

$$\delta_{th} = \int_H T_M(h) \cdot M(h) dh + \int_H T_G(h) \cdot G(h) dh \tag{8}$$

where H is the dam's height, T_M and T_G are respectively the mean temperature and the temperature gradient across the thickness of the dam, and M and G are influence functions between the temperature at a given elevation h and the thermal displacement.

These influence functions depend on the mechanical and geometrical properties of the structure (including mechanical boundary conditions).

By considering T_M and T_G independent of the height, Eq. (8) can be simplified as follows:

$$\delta_{th} = T_M \cdot \underbrace{\int_H M(h)dh}_{A} + T_G \cdot \underbrace{\int_H G(h)dh}_{B} \tag{9}$$

This hypothesis is a strong hypothesis because the thermal loads are non-homogeneous on the upstream face of the dam. Indeed, both the thermal stratification of the retention lake water and the temperature discontinuity at the retention level (temperature difference between the parts of the upstream surface below and above the retention level) are responsible of non-homogeneous temperatures (mean and gradient) along the height. Moreover, the dam thickness evolves along its height yielding different thermal inertia. Although it is possible to account for the variation of T_M and T_G along the height, by introducing several variables T_M and T_G for different elevations, for statistical stability reasons (multi-collinearity) the number of explicative variables has to be limited, and some sort of "average values" of T_M and T_G are employed in this contribution. This strong assumption, already made in the previous HSTT method (for the lagged variable $\Delta\theta_R$) is kept in the new HST-Grad model, which focuses on the temperature gradient introduction.

As for HSTT, the mean temperature T_M (respectively the temperature gradient T_G) is split into a seasonal component $T_{M,S}$ (respectively $T_{G,S}$) and a deviation ΔT_M (respectively ΔT_G) to the seasonal component:

$$\delta_{th} = A \cdot (T_{M,S} + \Delta T_M) + B \cdot (T_{G,S} + \Delta T_G) \tag{10}$$

The displacements induced by the seasonal components of the mean temperature and of the temperature gradient are captured by the seasonal function of the model. Thus, by considering the constants A and B as statistical parameters adjusted by the model, the thermal part of the HST-Grad model can be written:

$$f_5(S, \Delta T_M, \Delta T_G) = f_3(S) + a_{10} \cdot \Delta T_M + a_{11} \cdot \Delta T_G \tag{11}$$

Compared to HSTT, only the thermal part of the model is changed. The final expression of the HST-Grad model is given by:

$$\delta = a_0 + f_1(t) + f_2(z) + f_5(S, \Delta T_M, \Delta T_G) + \varepsilon \tag{12}$$

In Eq. (12), the coefficients a_0 to a_{11} are statistically adjusted on measurement by the least square method. It is worth noting that only one statistical parameter is added in the model (in comparison to HSTT), which means that the improvement is more physical than mathematical.

In the new HST-Grad model, the lagged variables ΔT_M and ΔT_G are computed from upstream and downstream temperatures (T_{up} and T_{do}). The downstream temperature is the air temperature. Compared to HSTT, the upstream temperature is changed to account for water temperature and the reservoir retention level h_w (Eq. (13)).

$$T_{up} = \left(\frac{h_w}{H}\right) \cdot T_{water} + \left(1 - \frac{h_w}{H}\right) \cdot T_{air} \tag{13}$$

In this way, the upstream temperature is a weighted average of the air temperature and water temperature with respect to the retention level.

Upstream and downstream temperatures are split into upstream and downstream average seasonal temperatures ($T_{up,S}$ and $T_{do,S}$) and deviations to these seasonal averages (ΔT_{up} and ΔT_{do}). The displacement induced by the seasonal components of the upstream and downstream temperatures is seasonal and so, it is captured by the seasonal function. Thus, only the deviations are used to estimate the lagged variables ΔT_M and ΔT_G. These variables are computed according to the one-dimensional conductive heat-transfer problem described in Appendix B. The one-dimensional section used in the computation is not a geometrical section of the dam; it is a fictitious section whose thermal inertia is represented by the parameter T_0, adjusted statistically. So, the fictitious Section (1D medium) is as representative as possible of the whole dam. As a consequence, the parameter T_0 identified is a kind of average of the thermal inertia of all the dam sections accounting for the influence of each section temperatures on the displacement. The same statistical parameter T_0 is used to calculate both the mean temperature and the temperature gradient.

It is worth highlighting that the variable ΔT_M corresponds to the variable $\Delta\theta_R$ of the HSTT model in the sense that they both represent the mean temperature of a 1D medium representative of the whole dam. However, the two variables are slightly different. Indeed, $\Delta\theta_R$ is computed with air temperature applied on both sides of the 1D medium, whereas ΔT_M is computed with air temperature applied at the downstream side and the average between air and water temperatures accounting for the retention level applied at the upstream side.

In the proposed model, thermal loads are restricted to air and water temperatures. Nevertheless, solar radiation also plays a role in the thermal behaviour of the dam [19]. Although, the effect of solar radiation can be partially captured by the seasonal function, the method could easily be extended to consider explicitly solar radiation by increasing air temperature according to the orientation and sun exposure of the surfaces [17].

4. Finite element modelling: development of a heuristic case

To validate the performance of the HST-Grad model to deal with water temperature, a two dimensional thermo-mechanical model of a gravity dam is built using the finite element method. The dam modelled in this section is the Izourt dam (see Table 2 for the main characteristics). Considering that monoliths are not joined up, a plane-stress model can be adopted [20]. Only the central monolith of the dam is modelled in this study. Fig. 2 shows the mesh used for the simulations. It is worth noting that very thin elements are used near the boundaries (≃5 cm) so as to capture the effect of high frequency thermal loads. Transient simulations are performed with a time step of one day in order to be coherent with the temperature signals used in HSTT analysis. Moreover, this time step is a good compromise between computational effort and accuracy of the results. The material properties used for the simulations are given in Table 1. It is assumed that there is no temperature

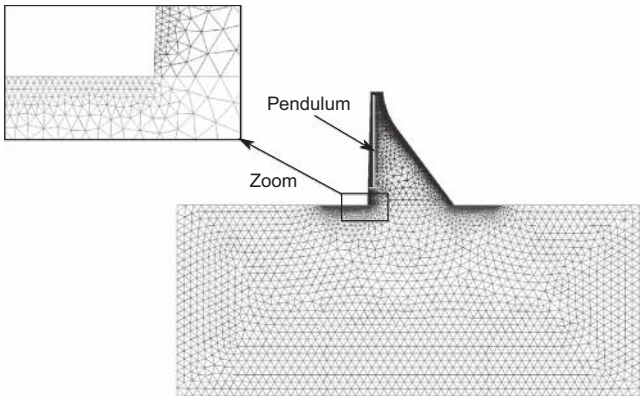

Fig. 2. Finite element mesh.

Table 1
Material properties.

	Poisson's ratio (–)	Density (kg/m^3)	Young modulus (GPa)	Coefficient of thermal expansion (°C^{-1})	Thermal conductivity (W/m/°C)	Specific heat (J/kg/°C)
Concrete	0.2	2300	30	$8 \cdot 10^{-6}$	2.5	900
Rock	0.25	2700	15	$8 \cdot 10^{-6}$	3	800

dependence of these parameters. For the temperature range of the dam, the conductivity and specific heat dependence on temperature have a negligible effect on the temperature prediction [21].

The mechanical boundary conditions define the embedding of the foundation. The normal component of the displacement vector is null along the foundation boundaries. Concerning the thermal boundary conditions, a zero heat flux condition is applied at the boundaries of the foundation. The air temperature or the water temperature are applied on the other boundaries of the model according to the retention level (to simplify the study, only air and water temperatures are accounted for in this numerical model).

The air temperature signal used in this model is the signal for a dam located in France at 1600 m of altitude. In absence of air temperature measurement available at the dam location, air temperature is modelled by interpolation of temperatures measured at several surrounding meteorological stations [22]. The model takes into account altitudinal gradients (dependent on season and rain) and gives the daily mean temperature at the dam location. Concerning the water temperature, a theoretical model is used (Eq. (14)). This model has been proposed by Bofang and Zhanmei [23] and improved by Ardito et al. [24].

$$T_w(y_w, t) = T_{bot}(t) \cdot \frac{1 - e^{-\Phi \cdot y_w}}{1 - e^{-\Phi \cdot H}} + T_{top}(t) \cdot \frac{e^{-\Phi \cdot y_w} - e^{-\Phi \cdot H}}{1 - e^{-\Phi \cdot H}} \tag{14}$$

In Eq. (14), $T_{bot}(t)$ and $T_{top}(t)$ are the signal of temperature at the bottom and at the top of the reservoir respectively, y_w is the depth under water surface, H is the height of the reservoir and Φ is a shape parameter. Because of the lack of water temperature measurements, the temperatures T_{bot} and T_{top} are considered as harmonic functions of the time (Eqs. (15) and (16)):

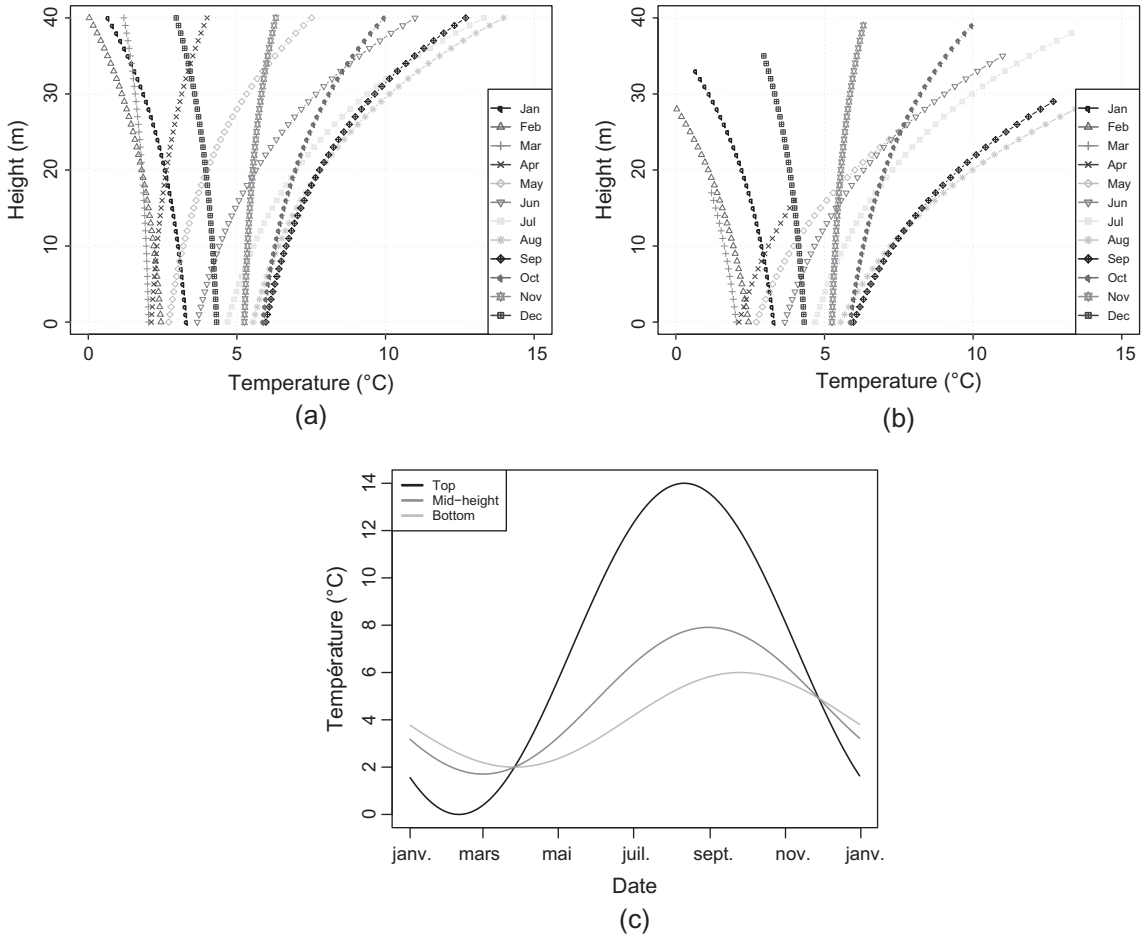

Fig. 3. Water temperature profiles for the different months of the year for a fixed retention level (a) and a variable retention level (b). Water temperature temporal variations at the top, mid-height and bottom of the reservoir for a fixed retention level (c).

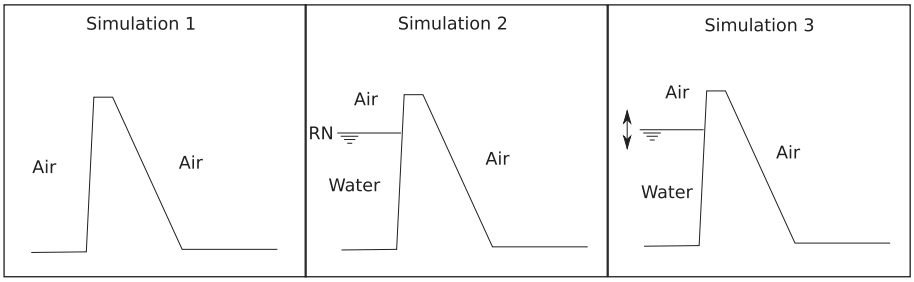

Fig. 4. Schematic representation of the thermal loads for the three simulations.

$$T_{top}(t) = 7 + 7 \cdot cos\left(2 \cdot \pi \cdot \frac{(t - \phi_{top})}{365}\right) \quad (15)$$

$$T_{bot}(t) = 4 + 2 \cdot cos\left(2 \cdot \pi \cdot \frac{(t - \phi_{bot})}{365}\right) \quad (16)$$

To account for the time delay due to heat transfer between air and water and in the water, the term ϕ_{top} (respectively ϕ_{bot}) is adjusted to insert a time delay of 15 days (respectively 60 days) between T_{top} (respectively T_{bot}) and the seasonal air temperature. The values of ϕ_{top} and ϕ_{bot} have been chosen arbitrarily. As the FE model is considered as a heuristic case, real values are not necessary for this study. The water temperature curves are given by Fig. 3. The water temperature follows a seasonal variation. Its amplitude decreases and its phase increases with depth.

It is known that the maximal water density is reached for a temperature of 4 °C [25] which means that water temperature profiles cannot cross the vertical lines at 4 °C. By construction, our model does not respect this condition, but only for a short period of the year.

Generally, due to mixing process, the reservoir warming period is longer than the cooling one, thus the water temperature variations are neither harmonic in time, nor exponential in space. The thermal evolution of a retention lake is highly dependent on several parameters: bathymetry of the reservoir, surface energy exchanges (air temperature, solar radiation, etc.), inflow and outflow (rivers, pumping, turbining, etc.), snow melting, ice cover at the top of the reservoir for dams in altitude or in northern regions (insulation from the cold air temperature). Thus, temperature measurements (at least at the surface and at the bottom of the reservoir) are necessary to have a precise time evolution of the lake thermal stratification. The lack of measurements leads us to employ harmonic temperatures in this study. Nevertheless, the FE model is used here as a heuristic case so that the precise time evolution of the real dam water temperature is not necessary.

To study the HSTT and HST-Grad performances, three simulations are performed with different combinations of the thermal loads (Fig. 4):

- *Simulation 1:* Only the air temperature is applied. The retention lake is empty.
- *Simulation 2:* Air and water temperatures are applied. The retention level is fixed at RN (normal value).
- *Simulation 3:* Air and water temperatures are applied. The retention level follows its real evolution (coming from in situ measurements).

Each simulation is performed over a period of 20 years but only the displacements of the last 10 years are analysed. Indeed, the first 10 years enable to reach a pseudo-harmonic steady state (the initial temperature field is uniform with a value equal to the air temperature average). Each simulation produces a series of displacements extracted from a virtual pendulum (Fig. 2) in the finite element model.

5. Validation of the HST-Grad model

5.1. Performance of the HST-Grad model to capture water temperature influence

For the three simulations (see Fig. 4), HSTT and HST-Grad but also classical HST analyses are performed on the ten-year displacement time series (the statistical calibration is performed over the period 2002–2012). Since only the thermal part of HSTT is modified in our original proposition, only temperature effect on dam displacements is analysed by means of finite element simulations and thus only the thermal part of the HST, HSTT and HST-Grad models is employed. Model efficiencies to capture the phenomena involved in the simulations are then evaluated using the residual dispersion as a criterion. The residual dispersion is defined in this study as the ratio (in %) between the standard deviation of the residuals and the amplitude of the displacement analysed. Since the statistical models are applied on finite element heuristic cases, residuals are only induced by model errors (there is neither measurement errors nor approximation of the input variables). Consequently, the lower the standard deviation is, the more efficient the model is. Fig. 5 shows the residual dispersion of the HST-Grad model compared to the ones of the HST and HSTT models for the three finite element simulations described in Section 4.

Moreover, Fig. 6 shows the relative importance of the mean temperature with respect to the temperature gradient on the thermally induced displacements determined by the HST-Grad model for the three simulations. The thermal displacements are considered here without the seasonal influences: $a_{10} \cdot \Delta T_M + a_{11} \cdot \Delta T_G$ in Eq. (11). The relative influence of one effect is measured by the

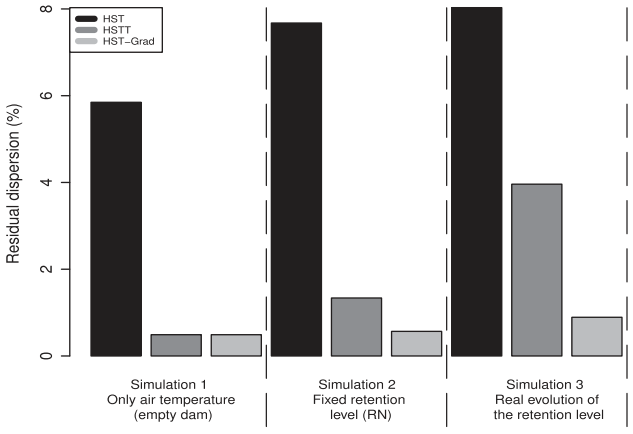

Fig. 5. HST, HSTT and HST-Grad residual dispersion for the three simulations.

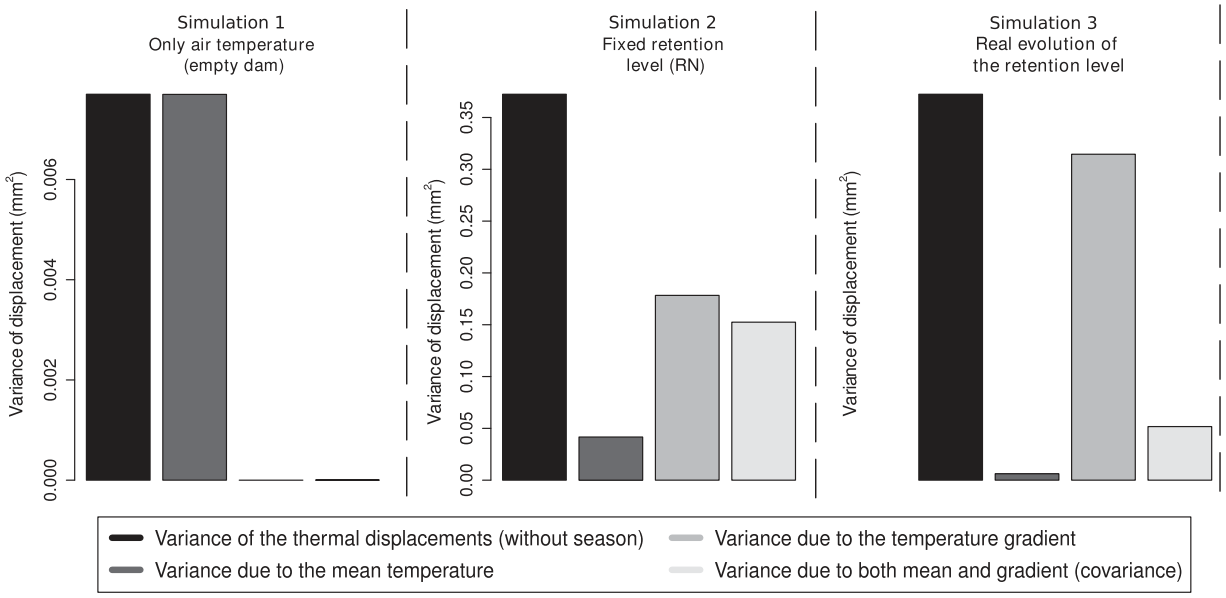

Fig. 6. Representation of the part of thermal displacements due to the mean temperature, to the gradient temperature or to both simultaneously (covariance) according to the HST-Grad model.

variance of its signal. By definition, the variance of the thermal displacements is the sum of the variance of the thermal displacement due to the mean temperature, the variance of the thermal displacement due to temperature gradient and twice the covariance of the two effects (Eq. (17)).

$$\underbrace{Var(a_{10}\cdot\Delta T_M + a_{11}\cdot\Delta T_G)}_{\text{variance of thermal displacement (without the seasonal influences)}} = \underbrace{Var(a_{10}\cdot\Delta T_M)}_{\text{variance of displacement due to mean temperature}} + \underbrace{Var(a_{11}\cdot\Delta T_G)}_{\text{variance of displacement due to temperature gradient}} + 2\cdot\underbrace{Cov(a_{10}\cdot\Delta T_M, a_{11}\cdot\Delta T_G)}_{\text{covariance of the two effects}} \quad (17)$$

Firstly, it is interesting to note that for the three simulations the HSTT and HST-Grad models enable an important reduction of the residual dispersion compared to the HST model. With only a seasonal function, the HST model is not able appreciate precisely the thermal influence on displacement.

For the first simulation, Fig. 5 shows that the HSTT model presents a low dispersion (≃0.5% of the total displacement amplitude). Indeed, the HSTT model is designed to capture the effect of air temperature from the upstream and downstream surfaces and it is exactly the conditions of this particular simulation. Nevertheless, the dispersion is not equal to zero since the dam has a true geometry, i.e. the thickness varies along the height. In HSTT, a unique section with an equivalent thickness in the thermal viewpoint (parameter T_0 statistically determined) is considered representative of all the dam horizontal sections. In other words, the HSTT model assumes that the boundary conditions and the dam thickness do not vary with height. HSTT is therefore not able to consider the evolution of thermal inertia along the height of the dam. On the contrary to the HSTT hypothesis, the dam thickness evolves with height in the heuristic case, leading to a certain amount of residual dispersion. Moreover, HSTT considers a one dimensional heat transfer, whereas the heat transfer is, in reality, in 3 directions (2 in the finite element simulation), mainly close to the upper and lower boundaries of the dam. The HST-Grad model does not reduce further the dispersion. Indeed, the dam reservoir is empty in this simulation (no thermal gradient are generated inside the structure) and consequently the total thermal displacement is explained by the mean temperature (see Fig. 6).

It is worth highlighting that the introduction of water temperature (simulation 2) increases a lot the dispersion of the HSTT model (Fig. 5). Indeed, the residual dispersion is multiplied by a factor 2.7 compared to the first simulation. Furthermore, it is interesting to note that the total displacement amplitude has also increased from 1.5 mm in the first simulation to 6 mm in the second one, meanings that the introduction of water temperature has a strong influence on the total displacement. It is noticeable that the dispersion of HSTT is strongly reduced (residual dispersion divided by 2.2) by taking into account water temperature (HST-Grad model). As the retention level is constant in this simulation, the improvement is still limited because the thermal effect induced by the variation of the retention level is greater than the effect of water temperature itself (water temperature is perfectly seasonal for the three simulations). Moreover, in this case, the mean temperature and temperature gradient are quite correlated (high covariance in Fig. 6), and thus, the HSTT model can explain a part of the effect induced by the temperature gradient.

For the last simulation, Fig. 5 shows a significant increase of the HSTT residual dispersion (multiplied by a factor 3 compared to the simulation 2). Indeed, the upstream boundary condition is dependent on the retention level variations and the HSTT model is not designed to account for these variations since the air temperature is applied for both the upstream and downstream surfaces. Concerning the HST-Grad model, it can be observed that the residual dispersion has just slightly evolved compared to simulation 2. Hence, the HST-Grad model is able to account for the thermal effect induced by the variation of the retention level. This effect is now directly accounted for in the HST-Grad model through Eq. (13). It is also interesting to remark that, for this simulation, the dispersion reduction obtained by HST-Grad compared to HSTT is in the same order of magnitude than the dispersion reduction obtained by HSTT compared to HST. Moreover, it is noticeable in Fig. 6 that the effect of the temperature gradient is much more important than the effect the mean temperature (which is almost equal to zero).

To conclude on the performance of the proposed model, it must be reminded that HSTT is designed to capture the displacement of a dam in which the thermal fluxes are in one dimension and subject to air temperature only (the influences of the other phenomena are reduced to the seasonal function). The present analysis shows that the water temperature and the variation of the retention level are important sources of dispersion for HSTT. Moreover, in presence of water with varying retention level, the temperature gradient has more influence than the mean temperature. That is why the new HST-Grad model improves a lot the results of HSTT by enabling to account for the displacements induced by water temperature.

5.2. Performance of the HST-Grad model to separate the mean temperature and the temperature gradient influences

In this section, the capability of the HST-Grad model to properly separate the mean temperature and the temperature gradient influences is analysed for the simulation 3. By keeping the coefficients a_{10}, a_{11} and T_0 calibrated by the HST-Grad model and using the mean temperature and temperature gradient computed with the total upstream and downstream temperatures (not only the deviation components), the effect of the gradient and mean temperatures on the total displacement is rebuilt. To be able to evaluate if the two effects obtained are well separated, they have to be compared to references. References components are computed by means of the thermo-elastic reciprocal theorem [26,16].

According to the thermo-elastic reciprocal theorem, the mean temperature and the temperature gradient influences on thermal displacement can be deterministically separated by means of Eq. (8). The functions $M(h)$ and $G(h)$ are easily estimated through Eqs. (18) and (19) (see Appendix A for more details).

$$M(h) = \alpha \cdot L(h) \cdot \int_{\Lambda} tr\left(\bar{\bar{\sigma}}\right)_M(h,\lambda)\, d\lambda \tag{18}$$

$$G(h) = \alpha \cdot \frac{L(h)^3}{12} \cdot \int_{\Lambda} tr\left(\bar{\bar{\sigma}}\right)_G(h,\lambda)\, d\lambda \tag{19}$$

In Eqs. (18) and (19), α is the coefficient of thermal expansion of the dam material, $L(h)$ is the thickness of the dam at height h, λ is the curvilinear coordinate along the length and $tr(\bar{\bar{\sigma}}(h,\lambda))$ is the trace of the stress tensor $\bar{\bar{\sigma}}(h,\lambda)$ obtained for a unit force applied at the location and in the direction where the displacement is sought. These influence functions $M(h)$ and $G(h)$ are computed in the finite element model and shown in Fig. 7. These functions can be read as follows:

- For example, an increase of 1 °C of the mean temperature of a one-meter high slice at elevation 30 m will produce a thermal displacement of −0.006 mm.
- In the same way, an increase of 1 °C/m of the temperature gradient of a one-meter high slice at elevation 30 m will produce a thermal displacement of −0.1 mm.

Knowing the influence functions $M(h)$ and $G(h)$, the thermal displacement is rebuilt from the finite element temperature field by applying Eq. (8). At first glance, the method seems inappropriate for a gravity dam since the simplified expression of the thermal displacement given by Eq. (8) is based on the assumption is that the trace of the stress tensor evolves linearly in all horizontal cross sections when a unit force is applied where the displacement is seeking. If this assumption can be understood for thin arch dam (shell theory), it seems inadequate for thick structures like gravity dams. Nevertheless, a very good agreement between the FE model and the simplified model can be observed in Fig. 8. Indeed, one can check in Fig. 9 that the deviation of the trace of the stress tensor from the linear approximation remains quite small, even for a gravity dam.

The thermo-elastic reciprocal theorem method, once validated for our gravity dam, is used to determine the mean temperature and temperature gradient influences (Eq. (8)). These two components are considered in the following as the reference components. Fig. 10 shows that the displacements due to the mean temperature and to the temperature gradient estimated with the HST-Grad model match quite well with the reference influences (determined with the thermo-elastic reciprocal theorem). The standard deviation of the residuals (difference between the signal issued from the thermo-reciprocal theorem and the one issued from the HST-Grad model) is about 0.1 mm for the two components (mean and gradient) meaning that the influences are well separated by the HST-Grad model.

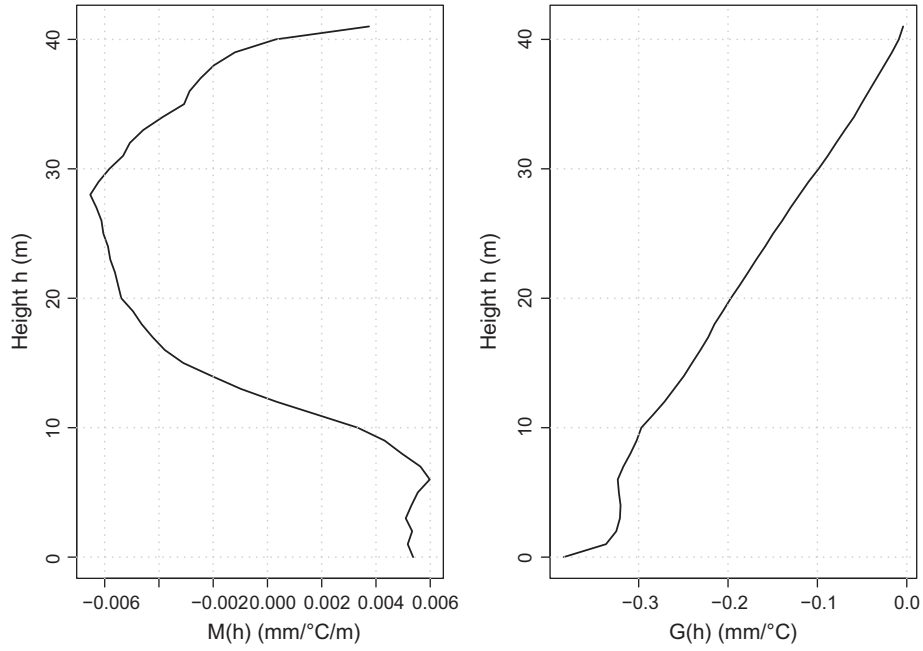

Fig. 7. Influence functions $M(h)$ and $G(h)$ for the mean temperature and the temperature gradient respectively.

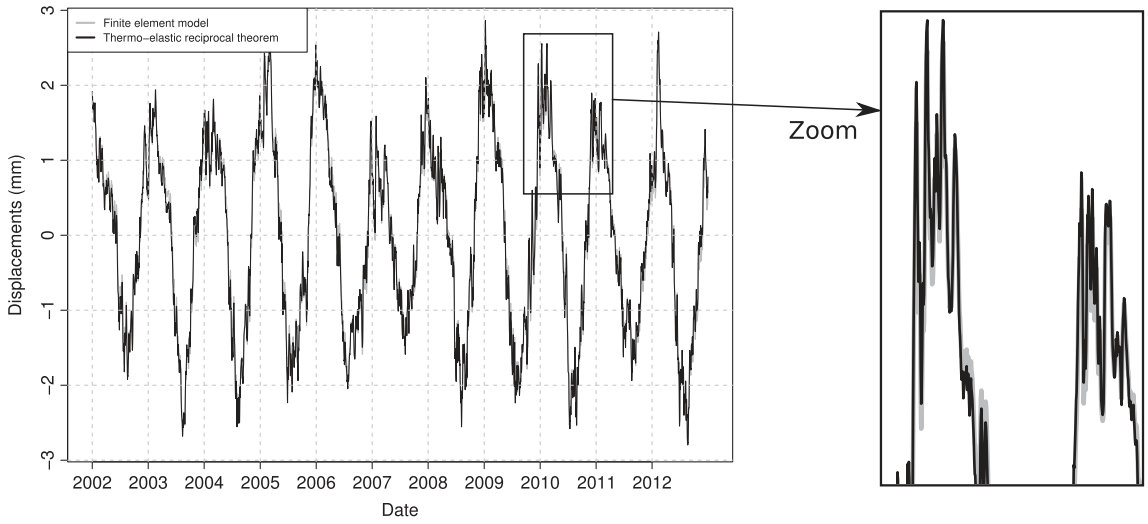

Fig. 8. Comparison of the displacement time series directly issued from the finite element simulation to the one computed with the thermo-elastic reciprocal theorem.

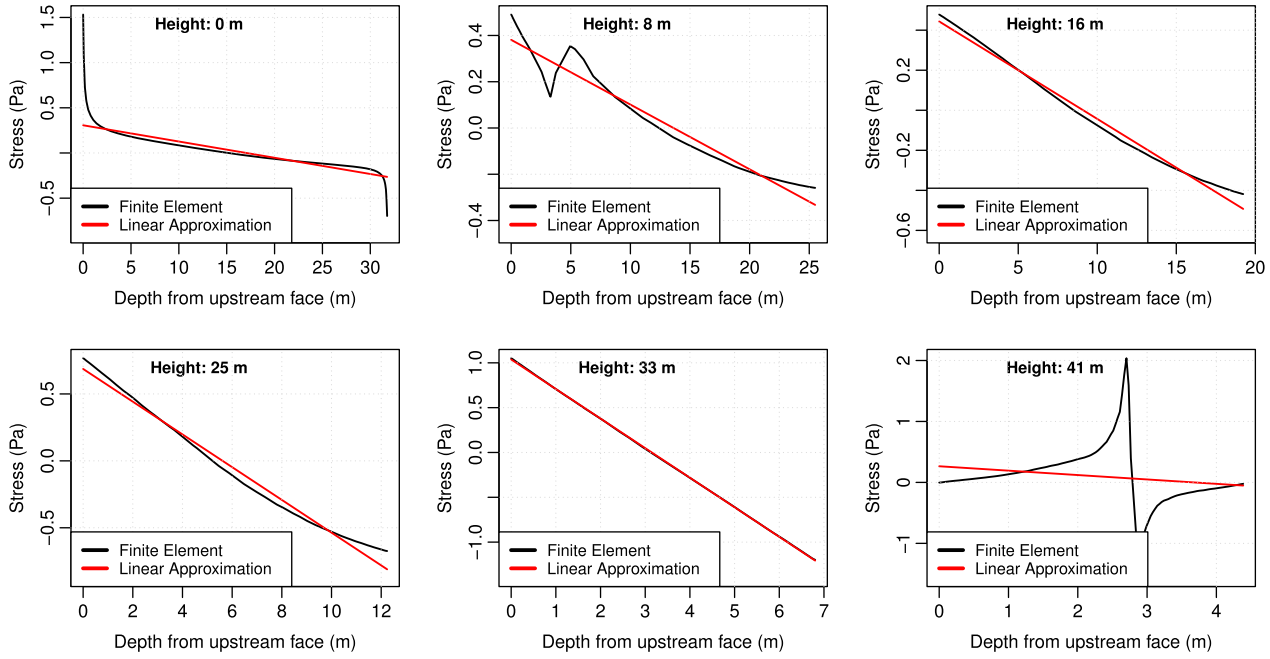

Fig. 9. Evolution of the trace of the stress tensor in the thickness of the dam for some horizontal cross sections.

Moreover, it is interesting to highlight that for this type of dam (gravity dam), the temperature gradient has much more influence on thermally induced displacement than the mean temperature (Fig. 10 shows that the amplitude of the temperature gradient influence is about 4 mm compared to less than 1 mm for the mean temperature influence).

5.3. Performance of the HST-Grad model on real cases

In this last part, the HST-Grad model is tested and compared to HSTT on real monitoring data. The analysis is performed for 8 French dams (see Table 2) over the period 2005–2013. The HSTT and HST-Grad models are calibrated over the period 2005–2012 and then used to forecast over the period 2012–2013.

In the finite element heuristic case, the water temperature is prescribed, however, for real cases, it is not known. For Izourt and Eguzon dams, water temperature has been measured over a period of one year, and then both signals have been approximated by one-year periodic functions and applied in the HST-Grad model (Fig. 11). It is noticeable in Fig. 11 that thermal behaviour of the two lakes are quite different. The real evolution of water temperature is not sinusoidal and depends on a lot of particular parameters which vary from one site to another. Nevertheless, for the other dams, some assumptions for the water temperature are necessary: water temperature is assumed to follow a perfect sinusoid of the time with a period one year, an amplitude of 4 °C and a mean of 7 °C, with a phase shift of one month compared to the seasonal air temperature. These values have been chosen arbitrarily and are consequently not fully representative of the real water temperature.

For each dam, the air temperature has been determined using an interpolation model [22]. This air temperature model

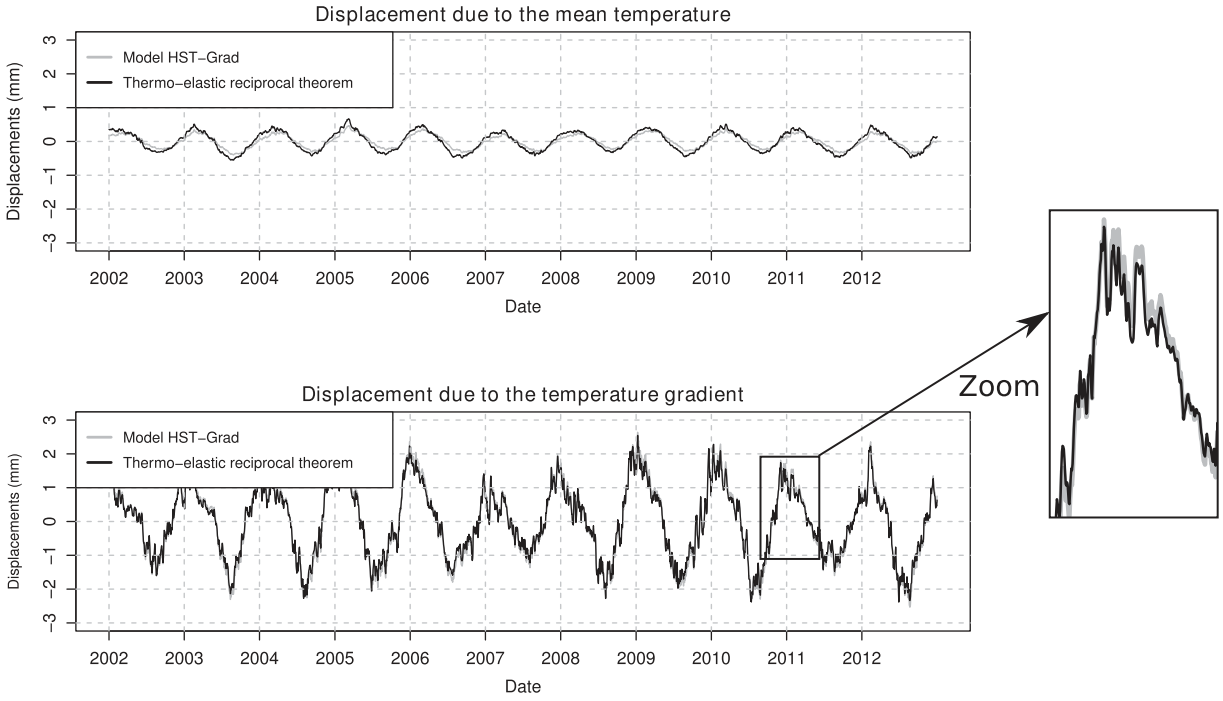

Fig. 10. Comparison of the displacement time series determined with the HST-Grad model to the one computed with the thermo-elastic reciprocal theorem – separation of the influence of the mean temperature and of the temperature gradient.

Table 2
Dams description.

Dam name	Type	Height (m)	Crest length (m)	Thickness at the top (m)	Thickness at the bottom (m)	Radius (m)	RN (m NGF)
Eguzon	Curved gravity dam	61	300	5	54	250	203
Izourt	Rectilinear gravity dam	44	162	4	28	–	1645
Roselend	Arch dam with buttresses	128	804	3	22	127	1557
Tignes	Arch dam	160	296	10	44	150	1790
Vouglans	Double curvature arch dam	127	425	6	25	107	429
Bissorte	Rectilinear gravity dam	60	545	6	42	–	2082
Gittaz	Curved gravity dam	66	164	4	48	180	1562
Sarrans	Gravity dam, slightly curved	97	225	4	75	–	647

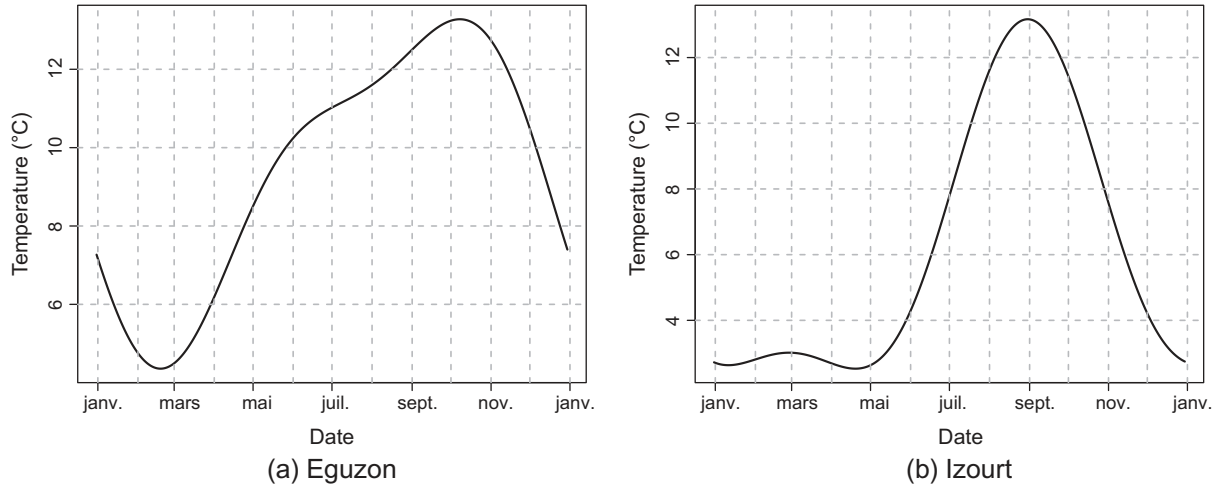

Fig. 11. Temporal evolutions of the mean water temperature measured in Izourt and Eguzon retention lakes over one year.

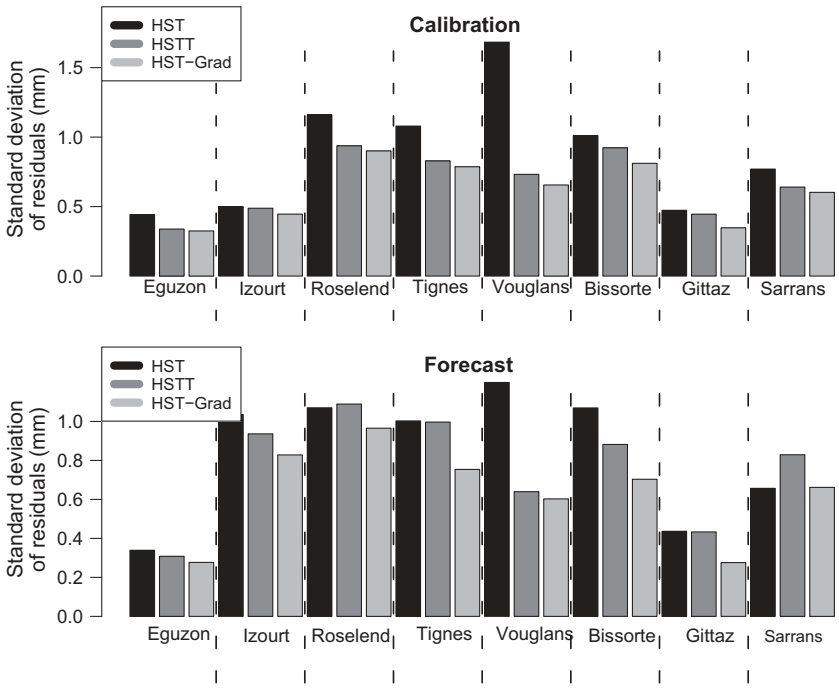

Fig. 12. HSTT and HST-Grad performances in terms of residual dispersion on eight French dams.

interpolates the measurements of several air temperature stations near the location of the dams and account for the weather type (rain, etc.) and the altimeter gradient.

Fig. 12 compares the performance of HST, HSTT and HST-Grad in terms of residual dispersion for both the calibration and the forecast. For all the tested dams, the HSTT model enables to reduce significantly the residual dispersion of the HST model on the calibration period. On the forecast period, the dispersion is not reduced for only two dams (Roselend, Sarrans). Moreover, one can notice that for all the dams, the HST-Grad model enables to reduce the residual dispersion of HSTT both in calibration and forecast. However, this improvement is not as important as expected with respect to the heuristic case. This can be explained by the low accuracy approximation of the environmental data (water and air temperatures) used to feed the model. Moreover the heuristic case considers uniquely air and water temperature. On real cases, other phenomena (solar radiation, etc.) are still not accounted for in the HST-Grad model and are also sources of the dispersion.

Nevertheless, one can remark that the improvement is more sensitive in forecasting which implies that the model has more physical sense and will lead to a better analysis of the irreversible part of the dam displacement.

5.4. Practical implementation of the HST-Grad model

For a practical computer implementation of the HST-Grad model, one needs at first the mean temperatures of the dam upstream and downstream faces T_{up} and T_{do}. Daily (or even hourly) measurements of air and water temperatures (or directly concrete temperatures near the dam faces) are necessary to feed efficiently the model. After a separation of the seasonal and unseasonal parts of the input signals T_{up} and T_{do}, the mean and gradient deviations ΔT_M and ΔT_G temperatures can then be computed from the unseasonal upstream and downstream temperatures ΔT_{up} and ΔT_{do} according to the recurrence formula given in Appendix B (Eqs. (B.16)–(B.21)). For numerical reasons, a finite number of terms has to be considered to compute the infinite sums (Eqs. (B.16) and (B.20)). If the input signals T_{up} and T_{do} are perfectly representatives of the dam behaviours, the more terms there are, the more accurate the solution is. Indeed, the more terms there are, the more the high frequencies of the input signals are accounted for. On the opposite, if the high frequencies of the input signals are not fully representatives of the dam behaviours, considering too much terms can deteriorate the solution. Moreover, for thin structures, more sensitive to high frequencies of thermal loads, a larger number of terms has to be considered. Thus, this number of terms has to be chosen according to several criteria: precision of the input signals, structure sensitivity to high frequencies of the thermal loads (dam width), and computational time allocated. If a good compromise has been found around 15 terms in this specific study, this number can vary in other situations. Besides, the time step Δt used for the computation of the recurrence formula has to be chosen according to the measurement frequency of the input signals T_{up} and T_{do}. Once the temperatures ΔT_{up} and ΔT_{do} are computed, the multi-linear regression can be performed (Eq. (12)). Then, the previous steps can be repeated with different values of the parameter T_0 until reaching the optimal value (dichotomous optimization process).

6. Conclusions

Based on the HSTT approach, an original hybrid physico-statistical model (called HST-Grad) has been developed to improve the assessment of displacements due to the temperature field in a dam. For this purpose, not only the air temperature is introduced in the model but also the water temperature so as to estimate the upstream temperature. Both the mean and the gradient of the temperature inside the structure could consequently be taken into account properly. These temperatures (mean and gradient) are estimated by analytically solving a one dimensional conductive heat transfer problem based on measured air and water temperature. Consequently, the water temperature profile is approximated by its mean value over the height and the evolution

of the retention level is accounted for with a upstream temperature equal to the weighted average of air and water temperature. Moreover, the thermal inertia of the one dimensional medium is adjusted to be representative of the whole dam.

The validation on a heuristic finite element model shows that the HST-Grad model enables us to reduce significantly the residual dispersion induced by water temperature and coupling between thermal boundary conditions and variation of the retention level. Indeed, the standard deviation of the residuals is divided by a factor 5 compared to the HSTT model. Moreover, the separation between the effect of the mean temperature and the temperature gradient has been validated and shows that the temperature gradient has more influence than the mean temperature on gravity dam displacements. On real cases, although the environmental data used to feed the model are approximations, a clear improvement is observed for both the calibration and the forecast. These results clearly indicate that the newly proposed model is more realistic, with only the cost of a measurement of the water temperature profile.

Although the proposed method shows a clear improvement, there is still the strong assumption that the temperatures (mean and gradient) are homogeneous along the height. A method accounting for non-homogeneous thermal loads and thermal inertia variation while limiting the multi-collinearity problem is currently under development.

Acknowledgment

3SR is part of the LabEx Tec 21 (Investissements d'Avenir – Grant agreement no. ANR-11-LABX-0030)

Appendix A. Calculation of thermal displacements

According to the thermo-elastic reciprocal theorem [26], the thermal displacements δ_{th} in any location and any direction of a concrete dam can be estimated through [16]:

$$\delta_{th} = \int_V \alpha \cdot T(h,l,\lambda) \cdot tr\left(\bar{\bar{\sigma}}(h,l,\lambda)\right) dv \tag{A.1}$$

where V is the dam's volume of concrete, h, l and λ are the space coordinates (along the vertical direction, along the horizontal radial direction and along the arcs (curvilinear coordinate) respectively (see Fig. 13) for notations), $dv = dh \cdot dl \cdot d\lambda$, α is the coefficient of thermal expansion, $T(h,l,\lambda)$ is the temperature field inside the dam and $tr(\bar{\bar{\sigma}}(h,l,\lambda))$ is the trace of the stress tensor $\bar{\bar{\sigma}}(h,l,\lambda)$ obtained for a unit force applied at the location and in the direction

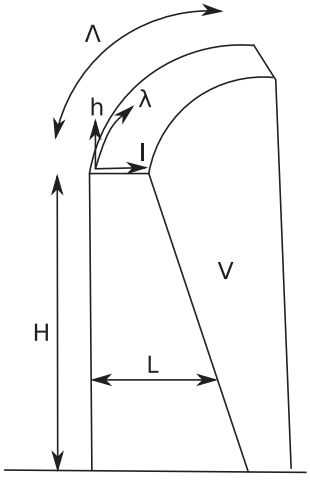

Fig. 13. Schematic representation of a dam with its geometrical variables.

where the displacements is sought. For example, to obtain the crest radial displacement of an arch dam, the unit force has to be applied at the crest (where the pendulum is anchored) in the radial direction.

According to Weber et al. [16], $tr(\bar{\bar{\sigma}})$ evolves linearly along the dam thickness (radial direction for an arch dam) if the dam is thin enough (shell theory). In this way, $tr(\bar{\bar{\sigma}})$ can be written as an approximation under the following form:

$$tr(\bar{\bar{\sigma}})(h,l,\lambda) \simeq tr(\bar{\bar{\sigma}})_M(h,\lambda) + \left(l - \frac{L}{2}\right) \cdot tr(\bar{\bar{\sigma}})_G(h,\lambda) \tag{A.2}$$

where L is the thickness, and $tr(\bar{\bar{\sigma}})_M$ and $tr(\bar{\bar{\sigma}})_G$ are respectively the mean and the gradient of $tr(\bar{\bar{\sigma}})$ along the thickness and are defined by:

$$tr(\bar{\bar{\sigma}})_M(h,\lambda) = \frac{1}{L} \cdot \int_0^L tr(\bar{\bar{\sigma}})(h,l,\lambda) dl \tag{A.3}$$

and,

$$tr(\bar{\bar{\sigma}})_G(h,\lambda) = \frac{12}{L^3} \cdot \int_0^L tr(\bar{\bar{\sigma}})(h,l,\lambda) \cdot \left(l - \frac{L}{2}\right) dl \tag{A.4}$$

Consequently, the integral along the thickness can be simplified as follow:

$$\begin{aligned} \int_L \alpha \cdot T \cdot tr(\bar{\bar{\sigma}}) dl &= \alpha \cdot tr(\bar{\bar{\sigma}})_M \cdot \int_0^L T dl + \alpha \cdot tr(\bar{\bar{\sigma}})_G \cdot \int_0^L T \cdot \left(l - \frac{L}{2}\right) dl \\ &= \alpha \cdot tr(\bar{\bar{\sigma}})_M \cdot L \cdot T_M + \alpha \cdot tr(\bar{\bar{\sigma}})_G \cdot \frac{L^3}{12} \cdot T_G \end{aligned} \tag{A.5}$$

where T_M and T_G are the mean temperature and the temperature gradient along the thickness respectively (Eq. (A.6)).

$$T(h,l,\lambda) \simeq T_M(h,\lambda) + \left(l - \frac{L}{2}\right) \cdot T_G(h,\lambda) \tag{A.6}$$

with,

$$T_M(h,\lambda) = \frac{1}{L} \cdot \int_0^L T(h,l,\lambda) dl \tag{A.7}$$

and,

$$T_G(h,\lambda) = \frac{12}{L^3} \cdot \int_0^L T(h,l,\lambda) \cdot \left(l - \frac{L}{2}\right) dl \tag{A.8}$$

By assuming that the mean temperature and the temperature gradient are constant for a given elevation ($T_M(h,\lambda) = T_M(h)$ and $T_G(h,\lambda) = T_G(h)$), Eq. (A.1) can be simplified as follow:

$$\delta_{th} = \int_H T_M(h) \cdot M(h) dh + \int_H T_G(h) \cdot G(h) dh \tag{A.9}$$

where H is the dam's height, and M and G are influence functions between the temperature at a given elevation h and the thermal displacement. These influence functions depend on the mechanical and geometrical properties of the structure (including mechanical boundary conditions):

$$M(h) = \alpha \cdot L(h) \cdot \int_\Lambda tr(\bar{\bar{\sigma}})_M(h,\lambda) d\lambda \tag{A.10}$$

$$G(h) = \alpha \cdot \frac{L(h)^3}{12} \cdot \int_\Lambda tr(\bar{\bar{\sigma}})_G(h,\lambda) d\lambda \tag{A.11}$$

Appendix B. Calculation of the mean temperature and temperature gradient across the dam

The mean temperature and the temperature gradient at a given elevation can be calculated through a one dimensional conductive

heat transfer problem (Eq. (B.1)), assuming that the upstream temperature T_{up} and downstream temperature T_{do} are known for this elevation.

$$\forall x \in [0,L], \forall t \in [0,+\infty[, D \cdot \frac{\partial^2 T}{\partial x^2}(x,t) - \frac{\partial T}{\partial t}(x,t) = 0 \tag{B.1}$$

$$T(0,t) = T_{up}(t) \quad \text{and} \quad T(L,t) = T_{do}(t) \tag{B.2}$$

In Eqs. (B.1) and (B.2), D is the thermal diffusivity and $T(x,t)$ is the temperature field inside the medium. The mean temperature $T_M(t)$ and the temperature gradient $T_G(t)$ of the medium can be calculated by means of convolution products of the signals $T_{up}(t)$ and $T_{do}(t)$ with the impulse responses for the mean temperature $P_M(t)$ and the temperature gradient $P_G(t)$ (see description below).

Eq. (B.4) gives the solution $S_1(x,t)$ of the 1D conductive heat transfer problem (Eqs. (B.1) and (B.2)) for step loads (Eqs. (B.1) and (B.2))

$$\begin{aligned} &T_{up}(t \leqslant 0) = 0; \quad T_{up}(t > 0) = T_{up} \quad \text{and} \quad T_{do}(t \leqslant 0) = 0; \\ &T_{do}(t > 0) = T_{do} \\ &\forall x \in [0,L], \forall t \leqslant 0 : S_1(x,t) = 0 \\ &\forall x \in [0,L], \forall t > 0 : \end{aligned} \tag{B.3}$$

$$\begin{aligned} S_1(x,t) = {} & \frac{2 \cdot T_{do}}{\pi} \cdot \sum_{n \geqslant 1} \frac{e^{-n^2 \cdot \frac{t}{T_0}}}{n} \cdot (-1)^n \cdot sin\left(\frac{n \cdot \pi \cdot x}{L}\right) \\ & - \frac{2 \cdot T_{up}}{\pi} \cdot \sum_{n \geqslant 1} \frac{e^{-n^2 \cdot \frac{t}{T_0}}}{n} \cdot sin\left(\frac{n \cdot \pi \cdot x}{L}\right) + T_{up} \cdot \left(1 - \frac{x}{L}\right) + T_{do} \cdot \frac{x}{L} \end{aligned} \tag{B.4}$$

In Eq. (B.4), T_0 is the characteristic time of the 1D medium (Eq. (B.5)) which accounts for the thermal inertia of the structure:

$$T_0 = \frac{L^2}{D \cdot \pi^2} \tag{B.5}$$

By differentiating the solution $S_1(x,t)$ with respect to time (the time derivative of a step is a pulse), one gets the solution $S_2(x,t)$ (Eq. (B.6)) of the 1D conductive heat transfer problem (Eqs. (B.1) and (B.2)) for a thermal pulse of weight T_{up} applied on the upstream side and another one of weight T_{do} applied on the downstream side at $t = 0$ ($T_{up}(t) = T_{up} \cdot \delta_{Dirac}(t)$ and $T_{do}(t) = T_{do} \cdot \delta_{dirac}(t)$ where $\delta_{Dirac}(t)$ is a Dirac pulse (Eq. (B.7)).

$$\begin{aligned} S_2(x,t) = \frac{dS_1}{dt}(x,t) = {} & T_{do} \cdot \delta_{Dirac}(t) \cdot \frac{2}{\pi} \cdot \sum_{n \geqslant 1} \frac{(-1)^n}{n} \cdot sin\left(\frac{n \cdot \pi \cdot x}{L}\right) \cdot e^{-n^2 \cdot \frac{t}{T_0}} \\ & - T_{up} \cdot \delta_{Dirac}(t) \cdot \frac{2}{\pi} \cdot \sum_{n \geqslant 1} \frac{1}{n} \cdot sin\left(\frac{n \cdot \pi \cdot x}{L}\right) \cdot e^{-n^2 \cdot \frac{t}{T_0}} \\ & - T_{do} \cdot \frac{2}{\pi} \cdot \sum_{n \geqslant 1} \frac{n \cdot (-1)^n}{T_0} \cdot sin\left(\frac{n \cdot \pi \cdot x}{L}\right) \cdot e^{-n^2 \cdot \frac{t}{T_0}} \\ & + T_{up} \cdot \frac{2}{\pi} \cdot \sum_{n \geqslant 1} \frac{n}{T_0} \cdot sin\left(\frac{n \cdot \pi \cdot x}{L}\right) \cdot e^{-n^2 \cdot \frac{t}{T_0}} + T_{do} \cdot \delta_{Dirac}(t) \cdot \frac{x}{L} \\ & + T_{up} \cdot \delta_{Dirac}(t) \cdot \left(1 - \frac{x}{L}\right) \end{aligned} \tag{B.6}$$

$$\delta_{Dirac}(t = 0) = +\infty; \quad \delta_{Dirac}(t \neq 0) = 0 \quad \text{and} \quad \int_{-\infty}^{+\infty} \delta_{Dirac}(t)dt = 1 \tag{B.7}$$

The mean temperature $S_M(t)$ and the temperature gradient $S_G(t)$ derived from $S(x,t)$ according to Eqs. (B.8) and (B.9):

$$\begin{aligned} S_M(t) = {} & \frac{1}{L} \int_0^L S_2(x,t)dx \\ = {} & \frac{(T_{up} + T_{do})}{2} \cdot \left(\left(1 - \frac{8}{\pi^2} \cdot \sum_{\substack{n \geqslant 1 \\ nodd}} \frac{e^{-n^2 \cdot \frac{t}{T_0}}}{n^2}\right) \cdot \delta_{Dirac}(t) \right. \\ & \left. + \frac{8}{\pi^2 \cdot T_0} \cdot \sum_{\substack{n \geqslant 1 \\ nodd}} e^{-n^2 \cdot \frac{t}{T_0}} \right) \end{aligned} \tag{B.8}$$

$$\begin{aligned} S_G(t) = {} & \frac{12}{L^3} \int_0^L S_2(x,t) \cdot \left(x - \frac{L}{2}\right) dx \\ = {} & (T_{do} - T_{up}) \cdot \left(\left(\frac{1}{L} - \frac{24}{\pi^2 \cdot L} \cdot \sum_{\substack{n \geqslant 1 \\ neven}} \frac{e^{-n^2 \cdot \frac{t}{T_0}}}{n^2}\right) \cdot \delta_{Dirac}(t) \right. \\ & \left. + \frac{24}{\pi^2 \cdot L \cdot T_0} \cdot \sum_{\substack{n \geqslant 1 \\ neven}} e^{-n^2 \cdot \frac{t}{T_0}} \right) \end{aligned} \tag{B.9}$$

The impulse response for the mean temperature $P_M(t)$ (Eq. (B.10)) is the mean temperature inside the medium for a unit average of the pulse applied at the two boundaries: $(T_{up} + T_{do})/2 = 1$ K. The impulse response for the gradient $P_G(t)$ (Eq. (B.11)) is the temperature gradient inside the medium for a unit difference of the pulses applied at the boundaries: $(T_{do} - T_{up}) = 1$ K.

$$P_M(t) = \left(1 - \frac{8}{\pi^2} \cdot \sum_{\substack{n \geqslant 1 \\ nodd}} \frac{e^{-n^2 \cdot \frac{t}{T_0}}}{n^2}\right) \cdot \delta_{Dirac}(t) + \frac{8}{\pi^2 \cdot T_0} \cdot \sum_{\substack{n \geqslant 1 \\ nodd}} e^{-n^2 \cdot \frac{t}{T_0}} \tag{B.10}$$

$$P_G(t) = \left(\frac{1}{L} - \frac{24}{\pi^2 \cdot L} \cdot \sum_{\substack{n \geqslant 1 \\ neven}} \frac{e^{-n^2 \cdot \frac{t}{T_0}}}{n^2}\right) \cdot \delta_{Dirac}(t) + \frac{24}{\pi^2 \cdot L \cdot T_0} \cdot \sum_{\substack{n \geqslant 1 \\ neven}} e^{-n^2 \cdot \frac{t}{T_0}} \tag{B.11}$$

The mean temperature $T_M(t)$ and the temperature gradient $T_G(t)$ inside the 1D medium for any real signals $T_{do}(t)$ and $T_{up}(t)$ are then obtained by the following convolution products:

$$T_M(t) = \int_0^\infty \frac{T_{up}(t-u) + T_{do}(t-u)}{2} \cdot P_M(u)du \tag{B.12}$$

$$T_G(t) = \int_0^\infty (T_{do}(t-u) - T_{up}(t-u)) \cdot P_G(u)du \tag{B.13}$$

By developing Eq. (B.12), it comes:

$$\begin{aligned} T_M(t) = {} & \int_0^\infty \frac{T_{up}(t-u) + T_{do}(t-u)}{2} \\ & \cdot \left(\left(1 - \frac{8}{\pi^2} \cdot \sum_{\substack{n \geqslant 1 \\ nodd}} \frac{e^{-n^2 \cdot \frac{u}{T_0}}}{n^2}\right) \cdot \delta_{Dirac}(u) + \frac{8}{\pi^2 \cdot T_0} \cdot \sum_{\substack{n \geqslant 1 \\ nodd}} e^{-n^2 \cdot \frac{u}{T_0}} \right) du \\ = {} & \int_0^\infty \frac{T_{up}(t-u) + T_{do}(t-u)}{2} \cdot \delta_{Dirac}(u)du \\ & - \frac{8}{\pi^2} \cdot \sum_{\substack{n \geqslant 1 \\ nodd}} \int_0^\infty \frac{T_{up}(t-u) + T_{do}(t-u)}{2} \cdot \frac{e^{-n^2 \cdot \frac{u}{T_0}}}{n^2} \cdot \delta_{Dirac}(u)du \\ & + \frac{8}{\pi^2 \cdot T_0} \cdot \sum_{\substack{n \geqslant 1 \\ nodd}} \int_0^\infty \frac{T_{up}(t-u) + T_{do}(t-u)}{2} e^{-n^2 \cdot \frac{u}{T_0}} du \end{aligned} \tag{B.14}$$

For any function of time $\Phi(t)$, $\int_0^\infty \Phi(t) \cdot \delta_{Dirac}(t)dt = \Phi(0)$. As a consequence, Eq. (B.14) becomes:

$$T_M(t) = \frac{T_{up}(t)+T_{do}(t)}{2} - \frac{8}{\pi^2}\cdot\sum_{\substack{n\geqslant 1\\ nodd}}\frac{T_{up}(t)+T_{do}(t)}{2}\cdot\frac{1}{n^2} + \frac{8}{\pi^2\cdot T_0}\cdot\sum_{\substack{n\geqslant 1\\ nodd}}\int_0^{\infty}\frac{T_{up}(t-u)+T_{do}(t-u)}{2}e^{-n^2\cdot\frac{u}{T_0}}du = \frac{T_{up}(t)+T_{do}(t)}{2}\cdot\left(1-\frac{8}{\pi^2}\cdot\sum_{\substack{n\geqslant 1\\ nodd}}\frac{1}{n^2}\right) + \frac{8}{\pi^2\cdot T_0}\cdot\sum_{\substack{n\geqslant 1\\ nodd}}\int_0^{\infty}\frac{T_{up}(t-u)+T_{do}(t-u)}{2}e^{-n^2\cdot\frac{u}{T_0}}du \quad (B.15)$$

Moreover, $\sum_{\substack{n\geqslant 1\\ nodd}}\frac{1}{n^2}=\frac{\pi^2}{8}$ and thus:

$$T_M(t) = \frac{8}{\pi^2\cdot T_0}\cdot\sum_{\substack{n\geqslant 1\\ nodd}}\int_0^{\infty}\frac{T_{up}(t-u)+T_{do}(t-u)}{2}e^{-n^2\cdot\frac{u}{T_0}}du = \frac{8}{\pi^2\cdot T_0}\cdot\sum_{\substack{n\geqslant 1\\ nodd}}X_n(t) \quad (B.16)$$

with:

$$X_n(t) = \int_0^{\infty}\frac{T_{up}(t-u)+T_{do}(t-u)}{2}e^{-n^2\cdot\frac{u}{T_0}}du \quad (B.17)$$

To compute the function $X_n(t)$ for a given value of n, the easiest way is to write it as a recursive formula. The following developments concern the establishment of the recursive formula. By writing $X_n(t+\Delta t)$, with Δt a time increment, one gets:

$$X_n(t+\Delta t) = \int_0^{\Delta t}\frac{T_{up}(t+\Delta t-u)+T_{do}(t+\Delta t-u)}{2}e^{-n^2\cdot\frac{u}{T_0}}du + \int_{\Delta t}^{\infty}\frac{T_{up}(t+\Delta t-u)+T_{do}(t+\Delta t-u)}{2}e^{-n^2\cdot\frac{u}{T_0}}du \quad (B.18)$$

It is assumed now that the temperature $T_{up}(t)$ and $T_{do}(t)$ are constant during the time interval Δt. In other words, $\forall v\in[t,t+\Delta t[: T_{up}(v)=T_{up}(t)$ and $T_{do}(v)=T_{do}(t)$. As a consequence, Eq. (B.18) becomes:

$$X_n(t+\Delta t) = \frac{T_{up}(t+\Delta t)+T_{do}(t+\Delta t)}{2}\cdot\int_0^{\Delta t}e^{-n^2\cdot\frac{u}{T_0}}du + \int_0^{\infty}\frac{T_{up}(t-w)+T_{do}(t-w)}{2}e^{-n^2\cdot\frac{w+\Delta t}{T_0}}du = \frac{T_{up}(t+\Delta t)+T_{do}(t+\Delta t)}{2}\cdot\frac{T_0}{n^2}\cdot\left(1-e^{-n^2\cdot\frac{\Delta t}{T_0}}\right) + e^{-n^2\cdot\frac{\Delta t}{T_0}}\cdot X_n(t) \quad (B.19)$$

In Eq. (B.19), the second term is obtained by substitution: $w=u-\Delta t$. Finally, the convolution product for the mean temperature (Eq. (B.12)) can be calculated by Eq. (B.16) in which each term of the sum is determined through the recurrence formula (Eq. (B.19)).

Following the same process for the gradient, it comes:

$$T_G(t) = \frac{24}{L\cdot\pi^2\cdot T_0}\cdot\sum_{\substack{n\geqslant 1\\ neven}}Y_n(t) \quad (B.20)$$

with,

$$Y_n(t+\Delta t) = \left(T_{do}(t+\Delta t)-T_{up}(t+\Delta t)\right)\cdot\frac{T_0}{n^2}\cdot\left(1-e^{-n^2\cdot\frac{\Delta t}{T_0}}\right) + Y_n(t)\cdot e^{-n^2\cdot\frac{\Delta t}{T_0}} \quad (B.21)$$

References

[1] Young P. Data-based mechanistic modelling of environmental, ecological, economic and engineering systems. Environ Model Softw 1998;13:105–22.
[2] Ferry S, Willm G. Méthodes d'analyse et de surveillance des déplacements observés par le moyen de pendules dans les barrages. In: VIth International congress on large dams. New-York; 1958. p. 1179–201 [in French].
[3] Willm G, Beaujoint N. Les méthodes de surveillance des barrages au service de la production hydraulique d'Èlectricité De France. In: IXth International congress on large dams. Istanbul; 1967. p. 529–50 [in French].
[4] Lugiez F, Beaujoint N, Hardy X. L'auscultation des barrages en exploitation au service de la production hydraulique d'Èlectricité De France, des principes aux résultats. In: Xth International congress on large dams. Montréal; 1970. p. 577–600 [in French].
[5] Post G. Dams and foundation monitoring. In: XVth International congress on large dams. Lausanne; 1985. p. 1623–727.
[6] Dibiagio E. Monitoring of dams and their foundations. In: XXth International congress on large dams. Beijing; 2000. p. 1459–545.
[7] Crépon O, Lino M. An analytical approach to monitoring. Int Water Power Dam Constr 1999:52–4.
[8] Guedes QM, Coelho PSM. Statistical behaviour model of dams. In: XVth International congress on large dams. Lausanne; 1985. p. 319–34.
[9] Silva Gomes AF, Silva Matos D. Quantitative analysis of dam monitoring results, state of the art, applications and prospects. In: XVth International congress on large dams. Lausanne; 1985. p. 749–61.
[10] Carrère AJ, Colson M, Goguel B, Noret C. Modelling: a means of assisting interpretation of readings. In: XXth International congress on large dams. Beijing; 2000. p. 1005–37.
[11] Chouinard L, Roy V. Performance of statistical models for analyzing the long term behaviour of dams. In: 2nd Conference on long term behaviour of dams. Graz; 2009. p. 141–6.
[12] OFITECO. Ausmodel 3.1 manual del usuario; 2011.
[13] Leger P, Leclerc M. Hydrostatic, temperature, time-displacement model for concrete dams. J Eng Mech 2007;133(3):267–77.
[14] Bossoney CL. Monitoring and back analysis: the importance of the temperature load case. Int J Hydropower Dams 1994;1(6):70–4.
[15] Weber B. Linear regression models for dam monitoring based on statistical analysis. In: Proceedings of the 6th international benchmark workshop on numerical analysis of dams, ICOLD. Salzburg; 2001. p. 70–4.
[16] Weber B, Perner F, Obernhuber P. Displacements of concrete dams determined from recorded temperatures. In: 8th ICOLD European club symposium. Innsbruck; 2010. p. 599–04.
[17] Stucky A, Derron MH. Problèmes thermiques posés par la construction des barrages-réservoirs, Paul Feissly; 1957.
[18] Penot I, Daumas B, Fabre JP. Monitoring behaviour. Int Water Power Dam Constr 2005:24–7.
[19] Tatin M, Briffaut M, Dufour F, Simon A, Fabre JP. Thermal displacements of concrete dams: Finite element and statistical modelling. In: 9th ICOLD European club symposium. Venice; 2013. p. B.24.
[20] Leger P, Venturelli J, Bhattacharjee SS. Seasonal temperature and stress distributions in concrete gravity dams. Can. J. Civ. Eng. 1993;20(6):999–1029.
[21] Briffaut M, Benboudjema F, Torrenti JM, Nahas G. Early age behaviour of a massive concrete structure: effects of thermal boundary conditions and thermal properties evolutions on temperature and stress fields. Eur. J. Environ. Civ. Eng. 2012;16(5):589–605.
[22] Gottardi F. Estimation statistique de réanalyse des précipitations en montagne. Utilisation d'ébauches par types de temps et assimilation de données d'enneigement. Application aux grands massifs montagneux français PhD thesis; Institut polytechnique de Grenoble; 2009 [in French].
[23] Bofang Z, Zhanmei L. External temperature loads. In: Laginha Seraphim J, Clough RW, editors. Arch dams. A.A. Balkema Publishers; 1990. p. 217–25.
[24] Ardito R, Maier G, Massalongo G. Diagnostic analysis of concrete dams based on seasonal hydrostatic loading. Eng Struct 2008;30:3176–85.
[25] Marsh KN. Recommended reference materials for the realization of physicochemical properties. Oxford: Blackwell Scientific Publications; 1987.
[26] Timoshenko SP, Goodier JN. Theory of elasticity. McGraw-Hill; 1970.